THE JOURNAL OF PHYSICAL CHEMISTRY Letters

Letter

pubs.acs.org/JPCL

Segmental Deuteration of α-Synuclein for Neutron Reflectometry on Tethered Bilayers

Zhiping Jiang,[†] Frank Heinrich,[‡,§] Ryan P. McGlinchey,[†] James M. Gruschus,[†] and Jennifer C. Lee*[,†]

[†]Laboratory of Protein Conformation and Dynamics, National Heart, Lung, and Blood Institute, National Institutes of Health, Bethesda, Maryland 20892, United States

[‡]Department of Physics, Carnegie Mellon University, Pittsburgh, Pennsylvania 15213, United States

[§]National Institute of Standards and Technology, Gaithersburg, Maryland 20899, United States

Supporting Information

ABSTRACT: Neutron reflectometry (NR) is uniquely suited for studying protein interaction with phospholipid bilayers along the bilayer normal on an angstrom scale. However, NR on its own cannot discern specific membrane-bound regions due to a lack of scattering contrast within a protein. Here we report the successful coupling of native chemical ligation (NCL) and NR to study α-synuclein (α-syn), a membrane-binding neuronal protein central in Parkinson's disease. Two α-syn variants were generated where either the first 86 or last 54 residues are deuterated, allowing for region-specific contrast within the protein and the identification of membrane interacting residues by NR. Residues 1−86 are positioned at the hydrocarbon/headgroup interface of the outer leaflet, whereas the density distribution of the 54 C-terminal residues ranges from the hydrocarbon region to the aqueous environment. Coupling of NCL and NR should have broad utility in studies of membrane protein folding.

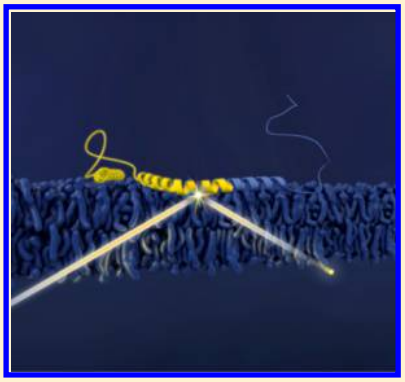

While neutron reflectometry (NR) is a widely used scattering technique to characterize interfacial thin-film properties,[1,2] its utility in membrane protein structure and biophysics is only developing. NR measurements are uniquely suited to evaluate the architecture of membrane proteins on lipid membrane bilayers and are able to provide information that is not available by other techniques. Using NR, the protein position and distribution profile normal to the membrane surface as well as the bilayer thickness changes upon protein binding can be measured on the angstrom scale.[3,4] Because of continued improvements in modeling approaches,[5] NR has been successfully applied to both peripheral and integral membrane proteins[6−14] and even protein complexes.[15,16]

The scattering length of neutron varies greatly between the isotopes of hydrogen, protium (^{1}H), and deuterium (^{2}H), with a much greater coherent scattering cross section for ^{2}H.[17] Thus deuteration of the protein of interest enhances contrast against the lipid bilayer membrane in an NR experiment.[3] However, protein perdeuteration does not provide spatial resolution of specific residues within the bilayer. The ability to assign specific polypeptide region within a protein distribution has yet to be realized by NR.

Here, through the coupling of native chemical ligation (NCL), we overcame this limitation in NR. This combined method allowed us to determine the location of membrane-bound residues within a sparsely tethered bilayer lipid membranes (stBLM)[18] for α-synuclein (α-syn), a membrane-binding neuronal protein central to the etiology of Parkinson's disease (PD). The ligation of uniformly deuterated portion (1−86 or 87−140) to the respective protiated segment (87−140 or 1−86) allowed for scattering contrast within the full-length α-syn. α-Syn serves an excellent example because its membrane interaction has been intimately associated with its biological and pathological function and elucidating its membrane interaction is crucial in understanding the cause of PD.[19−21]

NCL has been used in site-specific and isotopic labeling[22,23] of proteins as well as in installing posttranslational modifications.[24−27] The previously reported NCL constructs of α-syn, utilizing a short synthetic peptide (6−34 amino acids) and a larger fragment,[22,24−28] are not ideal for α-syn-membrane studies because the membrane binding region of α-syn encompasses the first 100 residues. Therefore, we created a new α-syn construct using recombinant protein fragments expressed from *E. coli*, which is advantageous by lowering cost and increasing yield. An NCL reaction requires an N-terminal Cys residue and a C-terminal thioester. Because α-syn has no native cysteine residues, site-directed mutagenesis was needed. To minimize change, Ser sites were considered and, out of the four native sites (9, 42, 87, 129), Ser87 was chosen to yield suitable peptide fragments (1−86 and 87−140) for *E. coli* expression with the 1−86 portion containing most of the lipid binding residues. Scheme 1 shows the NCL reaction of the segmentally deuterated α-syn. To avoid the spontaneous mutation Y136C in *E. coli*,[29] a silent codon change (TAC to TAT) was made at position 136. The deuterated portion was

Received: October 6, 2016
Accepted: December 7, 2016
Published: December 7, 2016

DOI: 10.1021/acs.jpclett.6b02304
J. Phys. Chem. Lett. 2017, 8, 29−34

Scheme 1. Segmental Deuteratation of α-Syn[a]

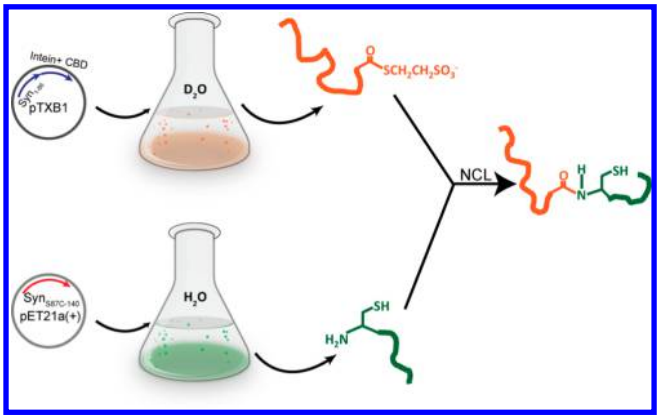

[a]N-terminus (Syn1−86) and C-terminus (S87C−140) were expressed in either D_2O- or H_2O-based media. The N-terminus construct contains a C-terminal Intein and Chitin binding domain (CBD). The C-terminus construct has an N-terminal Cys mutation. The purified N- and C-termini were chemically ligated to produce segmentally deuterated α-syn.

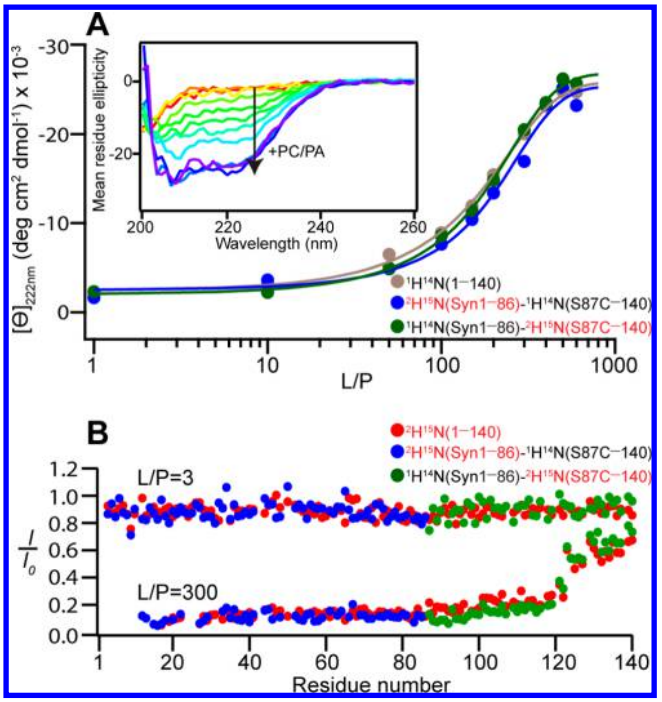

Figure 1. Binding of segmentally deuterated α-syn to equimolar PC/PA vesicles probed by CD and NMR spectroscopy. (A) Mean residue ellipticity at 222 nm ($[\Theta]_{222nm}$) is plotted against lipid-to-protein molar ratio (L/P) for fully protiated α-syn ($^1H^{14}N(1−140)$, gray), ligated N-terminal ($^2H^{15}N(Syn1−86)$-$^1H^{14}N(S87C−140)$, blue), and C-terminal ($^1H^{14}N(Syn1−86)$-$^2H^{15}N(S87C−140)$, green) deuterated α-syn. The peptide portion containing isotopic labeling is colored red in the legend text. Inset: Representative CD titration of 5 μM $^2H^{15}N(Syn1−86)$-$^1H^{14}N(87−140)$ with increasing PC/PA vesicles (0 to 3 mM, red-to-purple). (B) Comparison of HSQC intensity profiles of fully deuterated $^2H^{15}N(1−140)$ α-syn (red), $^2H^{15}N(Syn1−86)$-$^1H^{14}N(S87C−140)$ (blue), and $^1H^{14}N(Syn1−86)$-$^2H^{15}N(S87C−140)$ (green). Vesicles were made through extrusion (50 nm pore size) and measurements were taken at 25 and 15 °C for CD and NMR, respectively.

also uniformly labeled with ^{15}N for nuclear magnetic resonance (NMR) studies and is hereafter denoted as $^2H^{15}N$, and the protiated portion is denoted as $^1H^{14}N$. Experimental details regarding expression, purification, and ligation are provided in the Supporting Information. From a 1-L deuterated cell growth, the yield of ligated α-syn was 3−5 mg.

α-Syn membrane binding properties have been investigated by various biophysical techniques,[30−37] including NR.[6−8] Upon binding to membranes, the N-terminal 100 residues form an amphipathic α-helix, leaving the acidic C-terminal 40 residues unstructured and flexible in solution.[32,38−40] α-Syn has a preference for negatively charged membranes due to the electrostatic attraction from multiple lysine residues found in the N-terminal region, and the binding affinity is also modulated by the specific anionic phospholipid headgroup.[41] For this work, we chose an lipid composition of equimolar 1-palmitoyl-2-oleoyl-*sn*-3-glycero-phosphocholine and 1-palmitoyl-2-oleoyl-*sn*-3-glycero-phosphate (noted as PC/PA) because PC is the most abundant mammalian phospholipid, PA is the most strongly bound anionic lipid by α-syn,[30] and PC/PA has been well-studied in our lab.[6,7,35] Circular dichroism (CD) spectroscopy, which is highly sensitive to the presence of α-helical structure,[30,35] was used to confirm membrane binding by the segmentally deuterated α-syn. CD titrations were performed with PC/PA lipid vesicles made by extrusion (average diameter ∼90 nm). Extruded vesicles were employed because they have lower curvature and exhibit similar properties (e.g., comparable diffusion rate and defect density) to that of stBLM for NR experiments.[42] Figure 1A inset shows representative data for ligated α-syn with N-terminal deuteration ($^2H^{15}N(Syn1−86)$-$^1H^{14}N(S87C−140)$), where upon adding PC/PA vesicles, characteristic features for α-helical conformation develop. An isodichroic point at 202 nm indicates a two-state transition. Nearly identical binding profiles were observed for the isotopically labeled ligated variants compared with the WT protein, indicating similar membrane-binding affinities (Figure 1A).

In addition to CD spectroscopy, $^1H/^{15}N$ HSQC solution NMR spectra were acquired to examine the segmentally deuterated portions of α-syn, which were also ^{15}N-labeled. As expected, the HSQC spectra for the ligated variants showed small perturbations around residue 87 due to the Cys mutation compared with fully deuterated α-syn (Figure S1). The backbone amide (^{15}N) resonance intensity (I) in the presence of low (L/P = 3) and high (L/P = 300) concentrations of lipids was normalized to the intensity in the absence of lipids (I_0), and results are shown in Figure 1B. As α-syn associates with the slowly tumbling PC/PA vesicles, the NMR resonances of the vesicle-bound residues decrease in intensity, becoming undetectable.[40] The normalized ^{15}N intensity profiles are the same within error for deuterated full-length (red) and ligated N- (blue) and C-terminal (green) deuterated samples. At L/P = 3, minimal binding was observed, whereas at L/P = 300 the backbone amide intensity was reduced significantly for residues 1−100, and additional interaction was observed for residues 100 to 120, in accord with previous work.[39,40] Thus both CD and NMR data support the fact that segmental deuteration of α-syn does not change its membrane binding affinity and interacting residues.

NR measurements were performed on stBLM composed of equimolar PC/PA prepared by a vesicle fusion method,[7] where extruded vesicles were first adsorbed onto the self-assembled monolayer of tether molecules and then stBLM formation was induced by vesicle rupture and fusion through a rapid change of

DOI: 10.1021/acs.jpclett.6b02304
J. Phys. Chem. Lett. 2017, 8, 29−34

buffer osmolality (see SI for more details). To obtain the greatest contrast between phospholipids and membrane-bound residues, we first examined the ligated N-terminal deuterated α-syn. Representative reflectivity curves collected in the absence and presence of ligated N-terminal deuterated α-syn with two buffer contrasts from multiple measurements are shown in Figure 2A (top panel). Significant differences are observed in the Fresnel normalized reflectivity curves ($\Delta R/R_F$) upon the addition of ligated N-terminal deuterated α-syn up to 10 standard deviations (σ) at low momentum transfer Q_z values $\leq$0.15 Å^{-1} (lower panel in Figure 2A). Fitting the reflectivity curve with a monotonic Hermite spline yields the cross-section area distribution (volume occupancy) normal to the membrane and hence the membrane-associated protein density profile. Figure 2B shows the simplified molecular distributions for each interfacial layer of the stBLM obtained from the best global fit of all four reflectivity data. Consistent with previous NR results on full-length α-syn,[6,7] this profile shows that the majority of the protein resides in the outer leaflet, with some penetration into the hydrocarbon region of the bilayer. See Table S1 for all fit parameters.

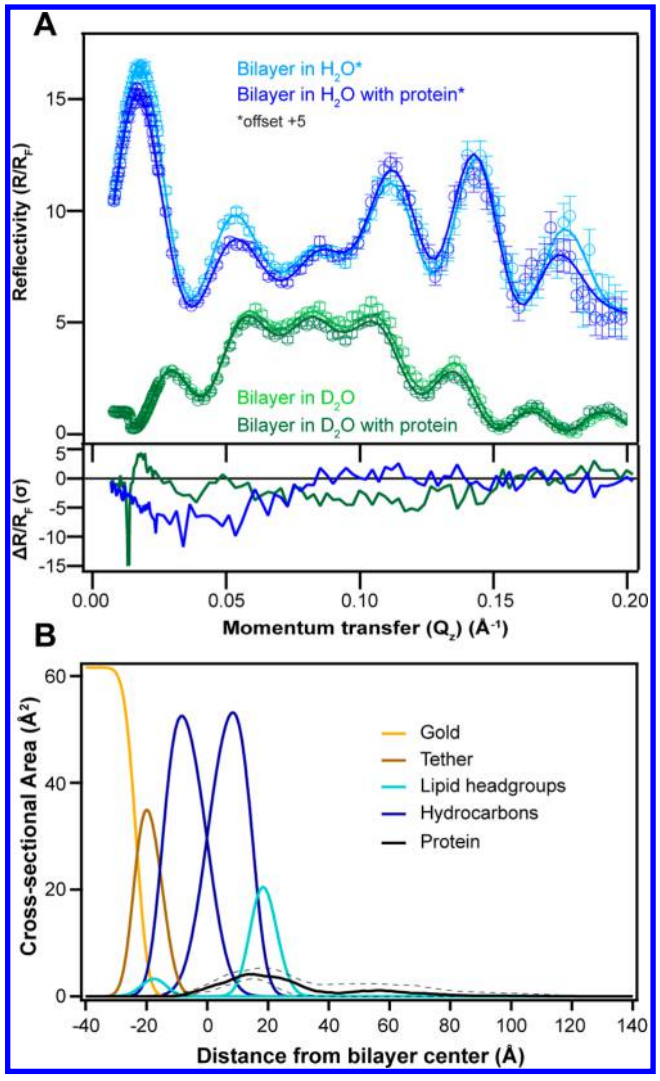

Figure 2. Ligated N-terminal deuterated α-syn membrane binding probed by NR. (A) Top panel shows neutron reflectivity (R/R_F) for equimolar PC/PA stBLM in the absence and presence of ligated α-syn with N-terminal deuteration (2 μM) in H_2O (blue) and D_2O (green) buffer (pH 7.0). Reflectivity curves in H_2O buffer are offset by five units for presentation clarity, marked as offset +5. Error bars represent 68% confidence intervals for the measured reflectivity based on Poisson statistics. Lower panel shows the differences between reflectivity curves ($\Delta R/R_F$) plotted in units normalized to the SD value (σ) of the experimental error. (B) Simplified molecular distributions for each interfacial layer of the PC/PA stBLM and ligated N-terminal deuterated α-syn. Median protein envelope is shown with 68% confidence interval (dark dashed lines). From left to right: gold (yellow), tether (brown), first layer lipid headgroups (cyan), first layer hydrocarbons (blue), second layer hydrocarbons (blue), and second layer lipid headgroups (cyan). Data for the Si substrate and the SiOx, Cr, and Au layer are partially omitted for simplicity.

Because of segmental deuteration, the protein distribution (Figure 3A) can be separated into the deuterated (residues 1−86, red) and protiated (residues 87−140, blue) portions (Figure 3B). As expected, the membrane-binding residues 1−86 have a relatively narrow distribution, with a maximum around the hydrocarbon-headgroup interface of the outer leaflet with negligible distribution in the bulk. In contrast, the density distribution of the 54-residue C-terminus is diffuse and ranges from the hydrocarbon region and up to ~60 Å into the bulk solvent. The presence of the protiated density in the bilayer could be due to binding of residues 87 to 100 and even possibly extending to residue 120.[40] There is greater uncertainty associated with the protiated portion due to its low volume occupancy of <2% at any given distance from the membrane. In addition to the protein distribution profile, NR is also able to provide membrane information, including thickness change upon protein binding. With the addition of ligated N-terminal deuterated α-syn, a small membrane thickening was detected (Table S1). Previous studies have shown that α-syn can induce small to moderate bilayer thinning or thickening.[6,7] An explanation of this variability has to await a comprehensive study on the effects of protein surface coverage, solution pH, and bilayer preparation.

To validate our assignment of membrane-interaction residues, NR measurements were performed on (1) the unligated deuterated N-terminal peptide (Syn1−86) and (2) the reverse segmentally deuterated α-syn construct (i.e., deuterated C-terminus with a protiated N-terminus, $^{1}H^{14}N$-(Syn1−86)-$^{2}H^{15}N$(S87C−140)). The reflectivity curves were collected (Figures S2 and S3), and the resulting membrane-associated protein density profiles are shown in Figure 3C−E. It is evident that the deuterated truncated Syn1−86 (Figure 3C) agrees well with the $^{2}H^{15}N$(Syn1−86) region of the segmentally deuterated α-syn (Figure 3B, red curve). The ligated C-terminal deuterated α-syn shows a smaller volume occupancy compared with that of N-terminal deuterated variant (~4 vs 6%), which results in greater uncertainty of the profile. The distribution profile is consistent with that obtained from the N-terminal deuterated protein. Colocalization of the C- and N-terminal regions is observed within the outer leaflet of the bilayer, albeit more prominently for the C-terminal deuterated protein (Figure 3E). For the two distributions, the amount of surface-associated protein is very close (~3 Å^3/Å^2) and so is the fraction of protein on the membrane (~64% including both hydrocarbon and headgroup regions). While the profile of ligated C-terminal deuterated α-syn shows more insertion into the hydrocarbon region of the bilayer, as indicated by the peak position at the membrane region compared with that of N-terminal deuterated form (5 vs 13 Å from the bilayer center (Figure 3A,D)), they are within error. Furthermore, it is not

DOI: 10.1021/acs.jpclett.6b02304
J. Phys. Chem. Lett. 2017, 8, 29−34

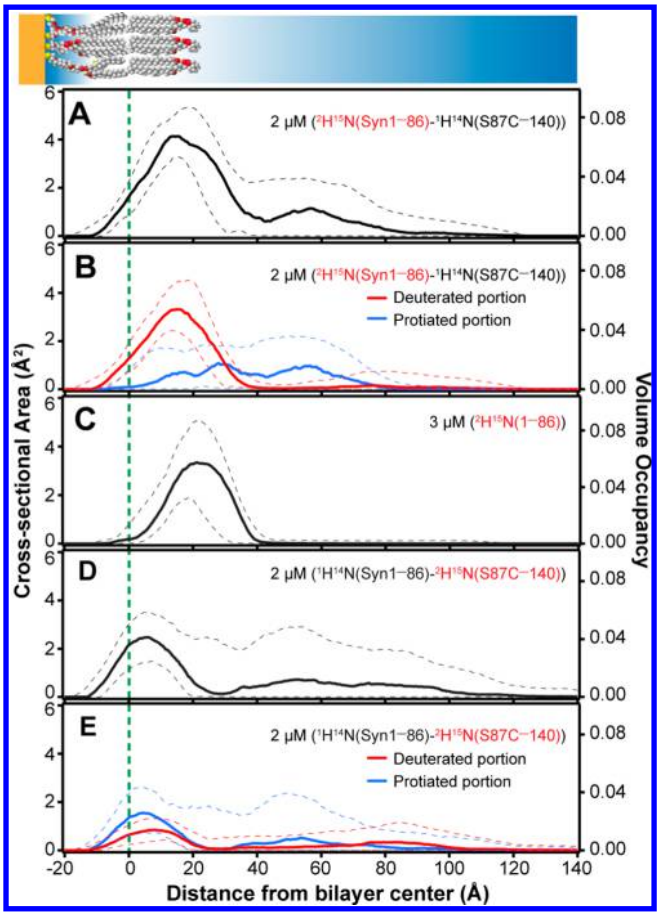

Figure 3. Distribution profile for ligated α-syn with equimolar PC/PA stBLM measured by NR. (A) Median protein envelope (solid line) for ligated N-terminal deuterated α-syn ($^{2}H^{15}N$(Syn1−86)-$^{1}H^{14}N$(S87C−140) obtained from the best fit of reflectivity data to the spline fit model is shown. The schematic drawing of lipid bilayer is shown on the top. (B) Deconvoluted individual distributions from panel A for the deuterated residues 1−86 and protiated residues 87−140 are shown in red and blue, respectively. For comparison, median protein envelopes (solid lines) for a C-terminal truncated Δ87−140 ($^{2}H^{15}N$(Syn1−86)) α-syn (C) and ligated C-terminal deuterated α-syn ($^{1}H^{14}N$(Syn1−86)-$^{2}H^{15}N$(S87C−140) (D) are shown. (E) Deconvoluted individual distributions from panel D for the protiated residues 1−86 and deuterated residues 87−140 are shown in blue and red, respectively. In all figures, the corresponding dashed lines represent 68% confidence intervals. Volume occupancy is indicated on the right axis. For ease of comparison, the green dashed line indicates the center of the bilayer. See Table S1 for all fit parameters.

feasible to directly compare their exact penetration depths as variations have been observed from individually prepared bilayers. Thus we consider the overall profiles of the two ligated α-syn as quite similar to each other, with most of the protein penetrating into the bilayer, while some protein density is observed in the bulk surrounding.

For completeness, we also examined the deuterated full-length WT (Figure S4), and unexpectedly we did not find any protein density in the proximal bulk solvent (>40 Å from bilayer center, Figure S4B), as we previously found for the protiated full length protein at pH 7.4,[6] but instead, it is similar to deuterated truncated Syn1−86 (Figure 3C) and previously reported deuterated full-length protein bound to PC/PA at pH 5.5.[7] In comparison with the segmentally deuterated samples, fully deuterated WT shows similar occupancy at the hydrocarbon region of the bilayer, but its protein density is moved from the bulk solvent into the headgroup region (Table S1), which implies that the C-terminal portion is residing much closer to the water/membrane interface. However, the differences between fully and segmentally deuterated α-syn were not observed by either CD or NMR spectroscopy. It is possible that the changes revealed by NR are too subtle to be detected by CD and NMR spectroscopy, as these methods inform on protein structure and are not sensitive to the context of relative bilayer position. However, with the current uncertainties and state of the technique, the density for the C-terminal portion for either ligated variants is not resolved with high enough confidence.

In summary, by using segmentally deuterated α-syn, we have for the first time identified region-specific protein−membrane interaction by NR. Our NR results reaffirm that NR is sensitive and well-suited for structural studies of membrane-associating proteins at the lipid/water interface. Not only is NR excellent in obtaining protein structural information along the *z* direction, normal to the membrane interface, but also by integrating the strategy of NCL, we believe that this will start an exciting new chapter on the applications of NR. We envision the ability to define both region-specific protein−lipid and intermolecular protein−protein interactions on a membrane surface. Furthermore, while the method of NCL has existed, it is not widely used because of the cost of peptide synthesis and inability to produce sufficient material for biophysical studies. Thus our detailed method to produce proteins by NCL with milligram yields not only is highly desirable for α-syn and NR but also applies to other intrinsically disordered proteins and techniques such as Raman, FTIR, and NMR spectroscopy.

■ ASSOCIATED CONTENT

Supporting Information

The Supporting Information is available free of charge on the ACS Publications website at DOI: 10.1021/acs.jpclett.6b02304.

Materials and methods, including expression and purification of chemically ligated α-syn, CD and NMR spectroscopy measurements, experimental details and analysis of neutron experiments, Table S1 with all NR fit parameters, and Figures S1−S4. (PDF)

■ AUTHOR INFORMATION

Corresponding Author

*Tel: +1(301) 496-3741. Fax: +1 (301) 402-3404. E-mail: leej4@mail.nih.gov.

ORCID

Jennifer C. Lee: 0000-0003-0506-8349

Notes

The authors declare no competing financial interest.

■ ACKNOWLEDGMENTS

This work is supported by the Intramural Research Program at the NIH, NHLBI and by the NIST IMS program "Precision Measurements for Integral Membrane Proteins". NR was performed on the NG-7 reflectometer at the NIST Neutron Center for Neutron Research and the NIST Center for Nanoscale Science and Technology. Parts of this research were performed at the NHLBI Biophysics (CD and DLS) and Biochemistry (ES-MS) Cores. We thank Nico Tjandra for the use of 800 MHz Bruker spectrometer. Certain commercial

DOI: 10.1021/acs.jpclett.6b02304
J. Phys. Chem. Lett. 2017, 8, 29−34

materials, equipment, and instruments are identified in this work to describe the experimental procedure as completely as possible. In no case does such an identification imply a recommendation or endorsement by NIST, nor does it imply that the materials, equipment, or instrument identified are necessarily the best available for the purpose.

REFERENCES

(1) Penfold, J.; Thomas, R. K. The Application of the Specular Reflection of Neutrons to the Study of Surfaces and Interfaces. *J. Phys.: Condens. Matter* **1990**, *2*, 1369−1412.

(2) Fragneto-Cusani, G. Neutron Reflectivity at the Solid/Liquid Interface: Examples of Applications in Biophysics. *J. Phys.: Condens. Matter* **2001**, *13*, 4973−4989.

(3) Heinrich, F. Deuteration in Biological Neutron Reflectometry. *Methods Enzymol.* **2016**, *566*, 211−230.

(4) Clifton, L. A.; Neylon, C.; Lakey, J. H. Examining Protein-Lipid Complexes Using Neutron Scattering. *Methods Mol. Biol.* **2013**, *974*, 119−150.

(5) Heinrich, F.; Losche, M. Zooming in on Disordered Systems: Neutron Reflection Studies of Proteins Associated with Fluid Membranes. *Biochim. Biophys. Acta, Biomembr.* **2014**, *1838*, 2341−2349.

(6) Pfefferkorn, C. M.; Heinrich, F.; Sodt, A. J.; Maltsev, A. S.; Pastor, R. W.; Lee, J. C. Depth of α-Synuclein in a Bilayer Determined by Fluorescence, Neutron Reflectometry, and Computation. *Biophys. J.* **2012**, *102*, 613−621.

(7) Jiang, Z.; Hess, S. K.; Heinrich, F.; Lee, J. C. Molecular Details of α-Synuclein Membrane Association Revealed by Neutrons and Photons. *J. Phys. Chem. B* **2015**, *119*, 4812−4823.

(8) Hellstrand, E.; Grey, M.; Ainalem, M.-L.; Ankner, J.; Forsyth, V. T.; Fragneto, G.; Haertlein, M.; Dauvergne, M.-T.; Nilsson, H.; Brundin, P.; et al. Adsorption of α-Synuclein to Supported Lipid Bilayers: Positioning and Role of Electrostatics. *ACS Chem. Neurosci.* **2013**, *4*, 1339−1351.

(9) Junghans, A.; Watkins, E. B.; Majewski, J.; Miranker, A.; Stroe, I. Influence of the Human and Rat Islet Amyloid Polypeptides on Structure of Phospholipid Bilayers: Neutron Reflectometry and Fluorescence Microscopy Studies. *Langmuir* **2016**, *32*, 4382−4391.

(10) Heinrich, F.; Nanda, H.; Goh, H. Z.; Bachert, C.; Loesche, M.; Linstedt, A. D. Myristoylation Restricts Orientation of the GRASP Domain on Membranes and Promotes Membrane Tethering. *J. Biol. Chem.* **2014**, *289*, 9683−9691.

(11) Le Brun, A. P.; Haigh, C. L.; Drew, S. C.; James, M.; Boland, M. P.; Collins, S. J. Neutron Reflectometry Studies Define Prion Protein N-terminal Peptide Membrane Binding. *Biophys. J.* **2014**, *107*, 2313−2324.

(12) Rondelli, V.; Brocca, P.; Motta, S.; Messa, M.; Colombo, L.; Salmona, M.; Fragneto, G.; Cantu, L.; Del Favero, E. Amyloid-β Peptides in Interaction with Raft-Mime Model Membranes: A Neutron Reflectivity Insight. *Sci. Rep.* **2016**, *6*, 20997.

(13) Erlkamp, M.; Moulin, J.-F.; Winter, R.; Czeslik, C. Packing Effects of N-Ras Binding to a DOPC Membrane - a Neutron Reflectivity and TIRF Spectroscopy High-Pressure Study. *Z. Phys. Chem.* **2014**, *228*, 969−986.

(14) McGillivray, D. J.; Valincius, G.; Heinrich, F.; Robertson, J. W. F.; Vanderah, D. J.; Febo-Ayala, W.; Ignatjev, I.; Loesche, M.; Kasianowicz, J. J. Structure of Functional Staphylococcus Aureus α-Hemolysin Channels in Tethered Bilayer Lipid Membranes. *Biophys. J.* **2009**, *96*, 1547−1553.

(15) Yap, T. L.; Jiang, Z.; Heinrich, F.; Gruschus, J. M.; Pfefferkorn, C. M.; Barros, M.; Curtis, J. E.; Sidransky, E.; Lee, J. C. Structural Features of Membrane-Bound Glucocerebrosidase and α-Synuclein Probed by Neutron Reflectometry and Fluorescence Spectroscopy. *J. Biol. Chem.* **2015**, *290*, 744−754.

(16) Clifton, L. A.; Johnson, C. L.; Solovyova, A. S.; Callow, P.; Weiss, K. L.; Ridley, H.; Le Brun, A. P.; Kinane, C. J.; Webster, J. R. P.; Holt, S. A.; et al. Low Resolution Structure and Dynamics of a Colicin-Receptor Complex Determined by Neutron Scattering. *J. Biol. Chem.* **2012**, *287*, 337−346.

(17) Jacrot, B. The Study of Biological Structures by Neutron Scattering from Solution. *Rep. Prog. Phys.* **1976**, *39*, 911−953.

(18) Budvytyte, R.; Valincius, G.; Niaura, G.; Voiciuk, V.; Mickevicius, M.; Chapman, H.; Goh, H.-Z.; Shekhar, P.; Heinrich, F.; Shenoy, S.; et al. Structure and Properties of Tethered Bilayer Lipid Membranes with Unsaturated Anchor Molecules. *Langmuir* **2013**, *29*, 8645−8656.

(19) Burre, J.; Sharma, M.; Tsetsenis, T.; Buchman, V.; Etherton, M. R.; Sudhof, T. C. α-Synuclein Promotes SNARE-Complex Assembly in Vivo and in Vitro. *Science* **2010**, *329*, 1663−1667.

(20) Dikiy, I.; Eliezer, D. Folding and Misfolding of α-Synuclein on Membranes. *Biochim. Biophys. Acta, Biomembr.* **2012**, *1818*, 1013−1018.

(21) Lashuel, H. A.; Overk, C. R.; Oueslati, A.; Masliah, E. The Many Faces of α-Synuclein: From Structure and Toxicity to Therapeutic Target. *Nat. Rev. Neurosci.* **2012**, *14*, 38−48.

(22) Batjargal, S.; Wang, Y. J.; Goldberg, J. M.; Wissner, R. F.; Petersson, E. J. Native Chemical Ligation of Thioamide-Containing Peptides: Development and Application to the Synthesis of Labeled α-Synuclein for Misfolding Studies. *J. Am. Chem. Soc.* **2012**, *134*, 9172−9182.

(23) Moran, S. D.; Woys, A. M.; Buchanan, L. E.; Bixby, E.; Decatur, S. M.; Zanni, M. T. Two-Dimensional IR Spectroscopy and Segmental C-13 Labeling Reveals the Domain Structure of Human γD-Crystallin Amyloid Fibrils. *Proc. Natl. Acad. Sci. U. S. A.* **2012**, *109*, 3329−3334.

(24) Hejjaoui, M.; Haj-Yahya, M.; Kumar, K. S. A.; Brik, A.; Lashuel, H. A. Towards Elucidation of the Role of Ubiquitination in the Pathogenesis of Parkinson's Disease with Semisynthetic Ubiquitinated α-Synuclein. *Angew. Chem., Int. Ed.* **2011**, *50*, 405−409.

(25) Hejjaoui, M.; Butterfield, S.; Fauvet, B.; Vercruysse, F.; Cui, J.; Dikiy, I.; Prudent, M.; Olschewski, D.; Zhang, Y.; Eliezer, D.; et al. Elucidating the Role of C-Terminal Post-Translational Modifications Using Protein Semisynthesis Strategies: α-Synuclein Phosphorylation at Tyrosine 125. *J. Am. Chem. Soc.* **2012**, *134*, 5196−5210.

(26) Fauvet, B.; Fares, M.-B.; Samuel, F.; Dikiy, I.; Tandon, A.; Eliezer, D.; Lashuel, H. A. Characterization of Semisynthetic and Naturally N-α-Acetylated α-Synuclein in Vitro and in Intact Cells Implications for Aggregation and Cellular Properties of α-Synuclein. *J. Biol. Chem.* **2012**, *287*, 28243−28262.

(27) Marotta, N. P.; Lin, Y. H.; Lewis, Y. E.; Ambroso, M. R.; Zaro, B. W.; Roth, M. T.; Arnold, D. B.; Langen, R.; Pratt, M. R. O-GlcNAC Modification Blocks the Aggregation and Toxicity of the Protein α-Synuclein Associated with Parkinson's Disease. *Nat. Chem.* **2015**, *7*, 913−920.

(28) Haj-Yahya, M.; Fauvet, B.; Herman-Bachinsky, Y.; Hejjaoui, M.; Bavikar, S. N.; Karthikeyan, S. V.; Ciechanover, A.; Lashuel, H. A.; Brik, A. Synthetic Polyubiquitinated α-Synuclein Reveals Important Insights into the Roles of the Ubiquitin Chain in Regulating Its Pathophysiology. *Proc. Natl. Acad. Sci. U. S. A.* **2013**, *110*, 17726−17731.

(29) Masuda, M.; Dohmae, N.; Nonaka, T.; Oikawa, T.; Hisanaga, S. I.; Goedert, M.; Hasegawa, M. Cysteine Misincorporation in Bacterially Expressed Human α-Synuclein. *FEBS Lett.* **2006**, *580*, 1775−1779.

(30) Davidson, W. S.; Jonas, A.; Clayton, D. F.; George, J. M. Stabilization of α-Synuclein Secondary Structure Upon Binding to Synthetic Membranes. *J. Biol. Chem.* **1998**, *273*, 9443−9449.

(31) Eliezer, D.; Kutluay, E.; Bussell, R.; Browne, G. Conformational Properties of α-Synuclein in Its Free and Lipid-Associated States. *J. Mol. Biol.* **2001**, *307*, 1061−1073.

(32) Jao, C. C.; Der-Sarkissian, A.; Chen, J.; Langen, R. Structure of Membrane-Bound α-Synuclein Studied by Site-Directed Spin Labeling. *Proc. Natl. Acad. Sci. U. S. A.* **2004**, *101*, 8331−8336.

(33) Nuscher, B.; Kamp, F.; Mehnert, T.; Odoy, S.; Haass, C.; Kahle, P. J.; Beyer, K. α-Synuclein Has a High Affinity for Packing Defects in a Bilayer Membrane - a Thermodynamics Study. *J. Biol. Chem.* **2004**, *279*, 21966−21975.

DOI: 10.1021/acs.jpclett.6b02304
J. Phys. Chem. Lett. 2017, 8, 29−34

(34) Ferreon, A. C. M.; Gambin, Y.; Lemke, E. A.; Deniz, A. A. Interplay of α-Synuclein Binding and Conformational Switching Probed by Single-Molecule Fluorescence. *Proc. Natl. Acad. Sci. U. S. A.* **2009**, *106*, 5645−5650.
(35) Pfefferkorn, C. M.; Lee, J. C. Tryptophan Probes at the α-Synuclein and Membrane Interface. *J. Phys. Chem. B* **2010**, *114*, 4615−4622.
(36) Middleton, E. R.; Rhoades, E. Effects of Curvature and Composition on α-Synuclein Binding to Lipid Vesicles. *Biophys. J.* **2010**, *99*, 2279−2288.
(37) Lokappa, S. B.; Ulmer, T. S. α-Synuclein Populates Both Elongated and Broken Helix States on Small Unilamellar Vesicles. *J. Biol. Chem.* **2011**, *286*, 21450−21457.
(38) Bussell, R.; Eliezer, D. A Structural and Functional Role for 11-Mer Repeats in α-Synuclein and Other Exchangeable Lipid Binding Proteins. *J. Mol. Biol.* **2003**, *329*, 763−778.
(39) Dikiy, I.; Eliezer, D. N-Terminal Acetylation Stabilizes N-Terminal Helicity in Lipid- and Micelle-Bound α-Synuclein and Increases Its Affinity for Physiological Membranes. *J. Biol. Chem.* **2014**, *289*, 3652−3665.
(40) Bodner, C. R.; Dobson, C. M.; Bax, A. Multiple Tight Phospholipid-Binding Modes of α-Synuclein Revealed by Solution NMR Spectroscopy. *J. Mol. Biol.* **2009**, *390*, 775−790.
(41) Pfefferkorn, C. M.; Jiang, Z.; Lee, J. C. Biophysics of α-Synuclein Membrane Interactions. *Biochim. Biophys. Acta, Biomembr.* **2012**, *1818*, 162−171.
(42) Shenoy, S.; Moldovan, R.; Fitzpatrick, J.; Vanderah, D. J.; Deserno, M.; Losche, M. In-Plane Homogeneity and Lipid Dynamics in Tethered Bilayer Lipid Membranes (tBLMs). *Soft Matter* **2010**, *6*, 1263−1274.

DOI: 10.1021/acs.jpclett.6b02304
J. Phys. Chem. Lett. 2017, 8, 29−34